Pump-probe spectroscopy with strong pulses as a tool to enhance weak electronic transitions

Maxim F. Gelin,[1] Andrey K. Belyaev,[2] and Wolfgang Domcke[1]
[1]*Department of Chemistry, Technische Universität München, D-85747 Garching, Germany*
[2]*Department of Theoretical Physics, Herzen University, St. Petersburg 191186, Russia*
(Received 27 February 2013; published 17 June 2013)

We show theoretically that pump-probe spectroscopy with strong pulses can be employed to effectively amplify weak electronic transitions and to learn about the associated material system dynamics. As an illustration, we discuss the possibility of the detection of weak transitions to discrete vibrational levels in the excited electronic state of the weakly bound He($2\,^1S$)-Ne dimer.

DOI: 10.1103/PhysRevA.87.063416 PACS number(s): 33.80.Wz, 82.53.−k

I. INTRODUCTION

Traditionally, atomic and molecular spectroscopy (in contrast to NMR spectroscopy) is performed with weak laser fields. In this regime, the probability of the light-induced transition from a certain initial system state $|i\rangle$ to a certain final state $|f\rangle$ is proportional, according to Fermi's Golden Rule, to $(\lambda\mu_{if})^2$ where λ is the amplitude of the external field and μ_{if} is the transition dipole moment. The intensity of the linear absorption or spontaneous emission scales thus with the square of the transition dipole moment.

In the weak-field limit, any four-wave mixing signal can be described as a product of four consecutive transitions, averaged over the initial states and summed over the intermediate and final states of the system [1]. If the strength of the fields increases, the system undergoes so-called ladder-climbing transitions involving up to several dozen system-field interactions [2–5]. These weak-field N-wave-mixing signals (within a certain spectral window) are dominated by transitions with large μ_{if}.

The situation changes qualitatively if the laser fields are so strong that the perturbative description of the system-field interaction is no longer valid. The rate of light-induced transitions is then determined by the corresponding Rabi frequency rather than Fermi's Golden Rule [6].

In steady-state spectroscopy, strong continuous wave (cw) pulses cause saturation of the optical transitions involved. This effect eliminates inhomogeneous (e.g., Doppler) broadening and yields narrow absorption lines of weak and otherwise undetectable transitions [6]. First demonstrated for the hyperfine splitting of the sodium D_1 and D_2 lines [7], saturation laser spectroscopy has been developed into a powerful technique for high-resolution atomic and molecular spectroscopy [8–14]. Four-wave-mixing saturation spectroscopy is nowadays an important diagnostic tool for measuring species concentrations and temperatures in flames and plasmas [15–18]. We mention also a recent experiment on magnetic dipole transitions in the $A\,^2\Sigma^+ \leftarrow X\,^2\Pi$ band system of the OH radical, in which electric dipole-allowed transitions are saturated by applying microwave pulses with a controlled duration and power [19].

In time-domain (femtosecond) spectroscopy, several groups have explored the phenomena induced by short and intense laser fields in various material systems, ranging from diatomic and polyatomic molecules [20–25] to biomolecules [26,27] and nano systems [28,29]. Several simulations of four-wave-mixing signals beyond the weak-pulse limit have been reported [30–41]. Strong-field control of molecular population transfer [42–44] and of other photophysical and photochemical processes ([45–50] and references therein) has been demonstrated. Single-molecule femtosecond spectroscopy [51] and control [52] also require strong pulses.

We propose herein that time-domain strong-field spectroscopy can be used for amplifying transitions with weak dipole moments. A preliminary argumentation goes like this. Consider a two-level system (ε_i and ε_f being the energy levels) excited by a laser pulse with the carrier frequency ω_p and duration τ_p. Assume that the system is in its lower state $|i\rangle$ before the arrival of the pump pulse. Then, after the pulse is over, the population of the upper state is (see, e.g., [6])

$$\varrho_{if} \equiv 2\left(\frac{\lambda\mu_{if}}{\Omega_R}\right)^2 [1-\cos(\Omega_R\tau_p)]. \tag{1}$$

Here $\Omega_R = \sqrt{(\varepsilon_i-\varepsilon_f-\omega_p)^2+4(\lambda\mu_{if})^2}$ is the Rabi frequency ($\hbar=1$). If $\Omega_R \gg |\lambda\mu_{if}|$ (which we call the weak-pulse regime), then $\varrho_{if} \sim (\lambda\mu_{if})^2 \ll 1$. If, on the other hand, $\Omega_R \approx 2|\lambda\mu_{if}|$ (which we call the strong-pulse regime), then $\varrho_{if} \approx [1-\cos(\Omega_R\tau_p)]/2$ and the system-field coupling is governed by Ω_R. If $\Omega_R\tau_p \approx \pi$ (so-called π pulse), the excited state is completely populated ($\varrho_{if}=1$) for a transition with any μ_{if}.

In the present paper, we suggest that pump-probe (PP) spectroscopy utilizing strong pulses may be a convenient tool to observe transitions with weak dipole moments, making them (metaphorically and literally) visible. We support our arguments by specific calculations of strong-pump strong-probe (SPSP) signals for the weakly bound HeNe dimer.

II. FORMULATION OF THE PROBLEM

The rare-gas dimers belong to the group of excimer molecules which are bound only in their excited states [53]. Several calculations performed in the 1990s predicted, however, that the electronic ground-state potential-energy function of the HeNe dimer can accommodate a single bound vibrational level [54,55]. Recently, accurate *ab initio* adiabatic potential-energy functions as well as several electronic transition dipole moments of the HeNe dimer have been calculated [56] for the ground state and excited electronic states up to 170 000 cm^{-1} excitation energy. Spin-orbit coupling effects were included through the use of a relativistic effective core

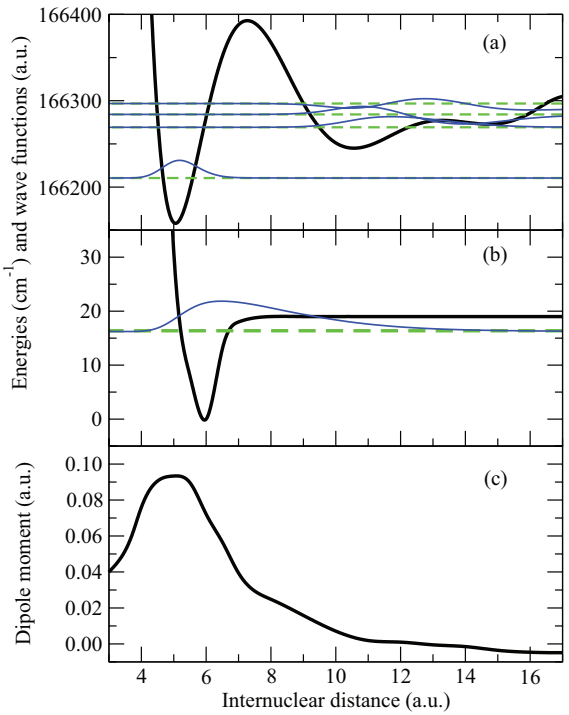

FIG. 1. (Color online) *Ab initio* adiabatic potential-energy curves for the HeNe dimer in the (a) ground state and (b) [He($2\,^1S$)-Ne] 0^+ excited state, along with (c) the corresponding transition dipole moment $\mu(R)$. Dashed green lines show the vibrational levels n, while thin blue lines depict the corresponding nuclear wave functions $\Psi_n(R)$, $n = 0,1,2,3,4$ [(a) and (b)].

potential for the Ne atom. The results of Ref. [56] have been improved in Ref. [57] for the ground state and the 0^+ excited electronic state asymptotically correlated to the He($2\,^1S$)-Ne interaction by carrying out additional calculations at the full configuration interaction limit.

The data for the electronic 0^+ states obtained in [57] are summarized in Fig. 1. Shown are the Born-Oppenheimer potential energy functions for the ground state [Fig. 1(b)] and the excited states [panel (a)], as well as the corresponding electronic transition dipole moment $\mu(R)$ [Fig. 1(c)] as functions of the internuclear separation R. The data predict the existence of four discrete vibrational levels n with the energies ε_n ($n = 1,2,3,4$) in the excited electronic state, as well as a single vibrational level 0 with energy ε_0 in the electronic ground state. The discrete levels (dashed lines) and the corresponding nuclear wave functions $\Psi_n(R)$ (thin solid lines) are depicted in Figs. 1(a) and 1(b). Once $\Psi_0(R)$, $\Psi_n(R)$, and $\mu(R)$ are known, we can evaluate the matrix elements of the transition dipole moment operator

$$\mu_{0n} = \int_0^\infty \Psi_0(R)\mu(R)\Psi_n(R)\,dR. \tag{2}$$

The values of ε_n and μ_{0n} are collected in Table I. It can be seen that $|\mu_{01}| \gg |\mu_{0n}|$, $n = 2,3,4$. This result can be immediately understood through the inspection of the wave functions $\Psi_n(R)$ [Figs. 1(a) and 1(b)] and the dipole moment $\mu(R)$ [Fig. 1(c)].

Although the *ab initio* data of Ref. [57] are more accurate than those of [56], the excited-state potential-energy function is uncertain at large internuclear distances. As shown in Fig. 1, the wave function $\Psi_1(R)$ of the lowest vibrational state of the electronic excited state is entirely localized in the interior well with a depth about 150 cm^{-1}. In contrast, the wave functions $\Psi_n(R)$ of the higher vibrational states ($n = 2,3,4$) are localized in the external van der Waals well with a depth of about 38 cm^{-1}. It has been pointed out in Ref. [57] that the depth of 38 cm^{-1} should be considered as a crude estimate due to the limitations of the multireference configuration interaction approach. It is therefore desirable to check experimentally whether the vibrational levels in the electronic excited state exist and to determine the depth of the exterior potential well. The problem is thus to detect the transitions to the excited-state levels n ($n = 2,3,4$) which are connected with the ground-state level 0 via very small μ_{0n}, while the intensity of the entire electronic transition is dominated by $|\mu_{01}|^2$. The HeNe dimer is thus a suitable model for the exploration of the application of SPSP spectroscopy.

III. EFFECTIVE HAMILTONIAN

As motivated in the previous section, we construct a five-level model Hamiltonian of the HeNe dimer in bra-ket notation as follows:

$$H = \sum_{n=0}^{4} |n\rangle \varepsilon_n \langle n|. \tag{3}$$

Here $n = 0$ corresponds to the single vibrational level ε_0 in the ground electronic state, while $n = 1,2,3,4$ refers to vibronic levels ε_n in the excited electronic state.

We consider electronically resonant transitions and employ the rotating-wave approximation (see [6] for the discussion of the validity of this approximation for strong pulses). The interaction of the system with the pump ($a = 1$) and probe ($a = 2$) pulses is then written as follows:

$$H_F(t) = -\sum_{a=1}^{2} [X^\dagger \mathcal{E}_a(t) + X\mathcal{E}_a^*(t)]. \tag{4}$$

Here

$$X \equiv \sum_{n=1}^{4} \mu_{0n} |0\rangle \langle n|, \tag{5}$$

μ_{0n} being the matrix elements of the transition dipole moment operator as defined by Eq. (2). The electric fields of the pulses ($a = 1,2$) are given by

$$\mathcal{E}_a(t) = \lambda_a E_a(t - \tau_a) \exp\{i(\mathbf{k}_a \cdot \mathbf{r} - \omega_a t)\}, \tag{6}$$

TABLE I. Vibrational energy levels ε_n, transition dipole moment matrix elements μ_{0n}, and lifetimes τ_n^e for the HeNe dimer.

n	ε_n (eV)	μ_{0n} (a.u.)	τ_n^e (s)
0	0.002		
1	20.607	3.65×10^{-2}	1.35×10^{-8}
2	20.615	7.96×10^{-4}	2.11×10^{-5}
3	20.617	1.15×10^{-3}	1.00×10^{-5}
4	20.618	8.37×10^{-4}	1.30×10^{-5}

where λ_a, $\mathbf{k}_a$, ω_a, $E_a(t)$, and τ_a denote the amplitude, wave vector, frequency, dimensionless envelope, and central time of the pulses. The values of ε_n and μ_{0n} are given in Table I.

It is convenient to reduce the energies in the excited electronic state and the carrier frequencies of the pulses by $\varepsilon = \varepsilon_1 - \varepsilon_0$. That is, we replace

$$\varepsilon_n \to \varepsilon_n - \varepsilon, \quad \omega_a \to \omega_a - \varepsilon. \tag{7}$$

This convention is used in the following.

The Liouville–von Neumann equation for the density matrix of the model dimer reads as

$$\partial_t \rho(t) = -i[H + H_F(t), \rho(t)]. \tag{8}$$

In general, the right-hand side of Eq. (8) has to be augmented with an operator $\Re\rho(t)$, which takes care of relaxation processes, dephasing effects, and finite lifetimes. However, all relevant relaxation channels (collisions of HeNe with buffer gas molecules, radiationless decays, etc.) occur on time scales which are much longer than that of the proposed SPSP experiment (see Sec. VI). The effect of $\Re$ can therefore be neglected.

IV. NONLINEAR POLARIZATION AND DOORWAY-WINDOW APPROXIMATION

The response of the system to the applied fields determines the total complex nonlinear polarization (angular brackets indicate the trace)

$$P(t) \equiv \left\langle X^\dagger \rho(t) \right\rangle = \sum_{\mathbf{k}} P_{\mathbf{k}}(t) e^{i\mathbf{k}\cdot\mathbf{r}}, \tag{9}$$

which contains contributions corresponding to all possible values of the wave vector

$$\mathbf{k} = l_1\mathbf{k}_1 + l_2\mathbf{k}_2 \tag{10}$$

(l_a are arbitrary integers). The PP polarization $P_{\rm PP}(t)$ obeys the phase-matching condition

$$l_1 = 0, \quad l_2 = -1. \tag{11}$$

The integral transient absorption PP (SPSP) signal is defined as [1,37]

$$S(T) = \mathrm{Im} \int_{-\infty}^{\infty} dt \mathcal{E}_2^*(t)[P_{\rm PP}(t) - P_{\rm PP}^{\rm off}(t)]. \tag{12}$$

Here $T \equiv \tau_2 - \tau_1$ is the time delay between the pump and probe pulses, and $P_{\rm PP}^{\rm off}(t) = P_{\rm PP}(t)|_{\lambda_1=0}$.

We assume that the pump and probe pulses are temporally well separated. In this case, the SPSP signal can be evaluated within the doorway-window (DW) approximation [1,58]. In the present case,

$$S(T) = \mathrm{Im}\left\{ W_{00} D_{00} + \sum_{n,m=1}^{4} W_{nm} e^{-i\omega_{nm}T} D_{mn} \right\}, \tag{13}$$

where $\omega_{nm} = \varepsilon_n - \varepsilon_m$ and the explicit expressions for the DW operators D and W are given in the Appendix.

In the simulations of PP signals, we use Gaussian pulses

$$E_a(t) = \exp\{-4\ln 2(t/\tau_p)^2\}, \tag{14}$$

τ_p being the pulse duration (full width at half maximum). Initially, the dimer is in its ground state $|0\rangle$. To compute the operators D [Eq. (A2)] and W [Eq. (A3)], the Liouville–von Neumann equation (8) is converted into matrix form by an expansion in terms of the eigenvectors $|n\rangle$ of the system Hamiltonian (3). The dynamics of the driven system is evaluated numerically exactly by the fourth-order Runge-Kutta integrator.

V. SPSP SIGNALS

Inspecting the matrix elements of the transition dipole moments of the HeNe dimer (see Table I), one recognizes that the transition to the lowest vibrational state of the excited electronic state possesses the strongest dipole moment μ_{01}. The remaining three dipole moments are weaker by factors of 45 (μ_{02}), 32 (μ_{03}), and 43 (μ_{04}). Therefore, the absorption spectrum of the model HeNe dimer is dominated by the strongest transition with the dipole moment μ_{01}. The same is true for the weak-pulse PP signal (not shown). It reflects the strongest transition only, rendering the Hamiltonian (3) an effective two-level ($|0\rangle$ and $|1\rangle$) system and rendering $S(T)$ time independent. Therefore, linear absorption spectroscopy and weak-pulse nonlinear spectroscopy cannot deliver information on the weak transitions.

The situation changes when strong pulses are used. If we assume that $\mu_{0n} = 0$ for $n = 2,3,4$, the SPSP signal is T independent, since no system dynamics is induced by the pulses. When the weak transition dipole moments are switched on, the SPSP signal exhibits nontrivial dynamics. This is illustrated in Fig. 2, which shows $S(T)$ (left panels) and their Fourier transforms $|S(\omega)|^2$ (right panels). Panels (a) correspond to nonzero μ_{02}, while $\mu_{03} = \mu_{04} = 0$. In this case, two upper vibronic levels in the excited electronic state can be probed. Despite $|\mu_{02}| \ll |\mu_{01}|$, $S(T)$ exhibits a beating with the frequency $\omega_{21} = \varepsilon_2 - \varepsilon_1 = 0.0073$ eV, which is clearly seen in the Fourier spectrum. Panels (b) correspond to nonzero μ_{02} and μ_{03}, while $\mu_{04} = 0$. In this case, the time evolution of $S(T)$ is more complex. The Fourier transform of $S(T)$ reveals two beating frequencies, ω_{21} and $\omega_{31} = \varepsilon_3 - \varepsilon_1 = 0.0091$ eV. If all dipole moments are nonzero, $S(T)$ exhibits more complex oscillatory behavior, and $|S(\omega)|^2$ shows three peaks corresponding to ω_{21}, ω_{31}, and $\omega_{41} = \varepsilon_4 - \varepsilon_1 = 0.0107$ eV [panels (c)]. Thus, SPSP spectroscopy not only enhances weak transitions, but also delivers quantitative information on the vibrational levels of the system.

Note that the relative amplitude of vibrational oscillations in Fig. 2 is comparatively low. If we define the contrast of the signal as

$$\Delta_S = |S_{\rm max}(T) - S_{\rm min}(T)|/|S_{\rm max}(T) + S_{\rm min}(T)|, \tag{15}$$

with $S_{\rm max}(T)$ and $S_{\rm min}(T)$ being the maximal and minimal values of $S(T)$, then $\Delta_S \approx 3\%$ for the transients in Fig. 2. A finer tuning of the amplitude, duration, and carrier frequency of the pump and probe pulses permits us to increase Δ_S and thus to improve the information content of the SPSP signal. This is illustrated in Fig. 3, which displays $S(T)$ calculated for the same parameters as in Fig. 2(c), except that the pulses are tuned into resonance with the second vibronic state $|2\rangle$. Clearly, the relative amplitude of beatings in Fig. 3 ($\Delta_S \approx 18\%$) is significantly higher than in Fig. 2(c).

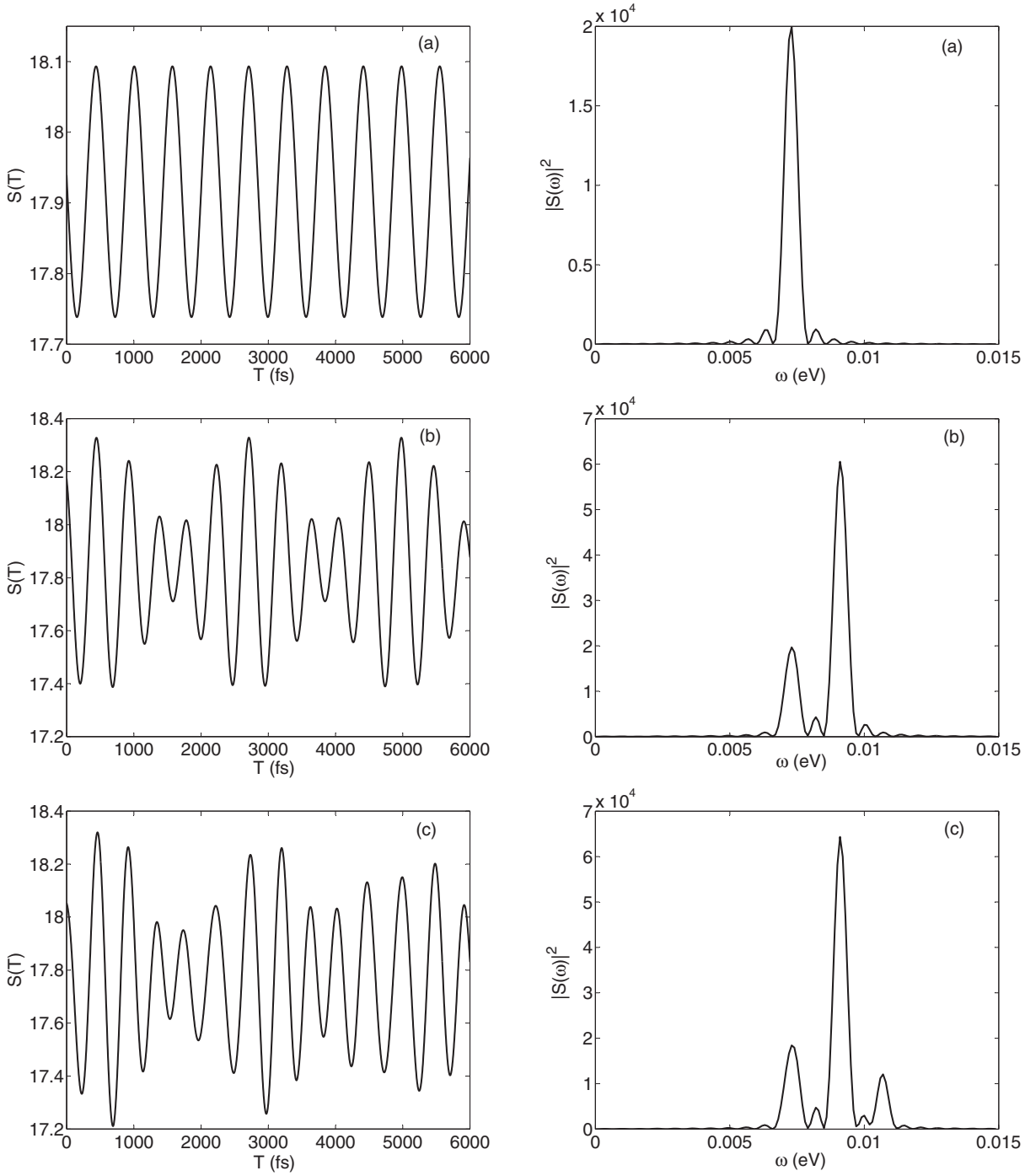

FIG. 2. SPSP signals $S(T)$ (left panels) and their Fourier transforms $|S(\omega)|^2$ (right panels) for strong ($\lambda\mu_{01} = 0.01$ eV) and relatively short ($\tau_p = 438$ fs) pulses with the reduced carrier frequencies $\omega_a = 0$. Panels (a): $\mu_{03} = \mu_{04} = 0$. Panels (b): $\mu_{04} = 0$. Panels (c): all μ_{0n} are nonzero.

VI. VALIDITY OF THE APPROXIMATIONS

The results illustrated by Figs. 2 and 3 are obtained by using the model Hamiltonian (3) and the dissipationless Liouville–von Neumann equation (8). The relevance of the underlying assumptions and their impact on the SPSP signals of the HeNe dimer is discussed below.

The radiative lifetimes of the excited vibronic states of the HeNe dimer were calculated in [57,59] and are collected in Table I. They fall into the nanosecond ($n = 1$) and microsecond ($n = 2,3,4$) time ranges. Their effect can therefore be neglected on the time scale of the SPSP experiment (a few picoseconds).

The dissociation energy of the lowest vibrational level 0 in the electronic ground state is estimated to be 0.45 meV [57,59]. To avoid collisional dissociation, the SPSP experiment should be performed at a temperature $T_{\rm eq}$ on the order of a few Kelvins.

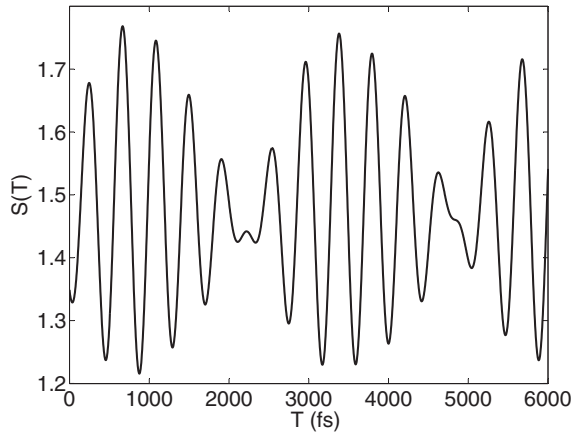

FIG. 3. Same as in Fig. 2(c), but for pulses with the reduced carrier frequencies $\omega_a = 0.007$ eV.

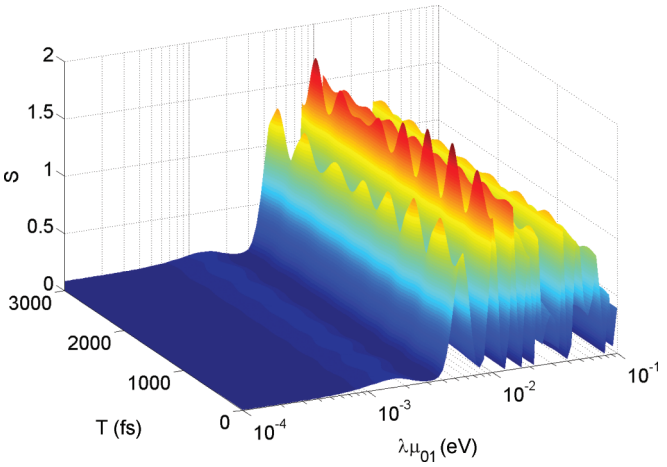

FIG. 4. (Color online) SPSP signal as a function of the interpulse delay T and the pulse amplitude $\lambda = \lambda_a, a = 1,2$. The duration ($\tau_p = 438$ fs) and the reduced carrier frequencies ($\omega_a = 0.007$ eV) of the pulses are fixed.

For $T_{\rm eq} = 1$ K, for example, $k_B T_{\rm eq} = 0.086$ meV (k_B is the Boltzmann constant).

We did not explicitly consider the averaging over the orientations of the transition dipole moments. It can be shown that the effect of orientational averaging is equivalent to an effective renormalization of the pulse strengths [38].

The characteristic time of molecular reorientation can be estimated as $\sqrt{I/(k_B T_{\rm eq})}$ (I is the moment of inertia). For HeNe in the ground electronic state at $T_{\rm eq} = 1$ K this yields 750 fs. To estimate the effect of rotation, we note that the SPSP signal can be split into the sum of isotropic (rotationally invariant) and anisotropic contributions. The former is unaffected by the molecular rotation, while the latter evolves to a stationary anisotropic distribution [60]. For a linear rotor like HeNe, the stationary anisotropy is smaller than the initial anisotropy by a factor of 4. Therefore, molecular reorientation will result in a partial reduction of $S(T)$.

VII. WHAT IS THE OPTIMAL FIELD STRENGTH?

Resolving weak transitions via SPSP spectroscopy requires a nonperturbative system-field interaction. In this regime, excitation and detection are implemented via multiple Rabi cycles of the material system within pump and probe pulses. To uncover the physical mechanisms of the amplification of weak transitions by strong pulses, Fig. 4 shows the SPSP signal as a function of the interpulse delay T and the pulse amplitude $\lambda_a \equiv \lambda$.

Consider first the SPSP signal vs λ for fixed T. It is seen that $S(\lambda)$ first rises, then reaches its first maximum at $\lambda\mu_{01} \approx 0.006$ eV and develops pronounced oscillations for higher values of λ. Thus, $\lambda\mu_{01} \approx 0.006$ eV marks the borderline between the weak-to-moderate pulse regime and the strong-pulse regime for the system under consideration. This behavior can be qualitatively explained by the consideration of Eq. (1). The intensity of the SPSP signal is given by $\sum_{i,f} |\varrho_{if}|^2$ [cf. Eq. (13)]. The weak-pulse regime corresponds to $\varrho_{if} \sim (\lambda\mu_{if})^2 \ll 1$. In this regime, the signal scales as $\sim\lambda^4$. In the strong-pulse regime, $\varrho_{if} \sim 1 - \cos(\Omega_R \tau_p)$. The SPSP signal is thus an oscillatory function of the pulse amplitude λ_a or the pulse duration τ_p.

As a function of T, the SPSP signal also shows two qualitatively different behaviors, see Fig. 4. For $\lambda\mu_{01} < 0.006$ eV (weak-to-moderate pulse regime), $S(T)$ does not exhibit pronounced dynamics. For $\lambda\mu_{01} > 0.006$ eV (strong-pulse regime), $S(T)$ develops pronounced vibrational beatings involving the system frequencies $\omega_{n1} = 0$ ($n = 2,3,4$). To detect these beatings, the Rabi periods $2\pi/\Omega_R$ must be comparable to (or shorter than) the pulse duration τ_p, both for the strong ($n = 1$) and weak ($n = 2,3,4$) transition dipole moments μ_{0n}. The contributions from all transitions are then comparable.

On the other hand, the inverse pulse duration should match characteristic system frequencies. We therefore used pulses with $\tau_p = 440$ fs in the simulations. Shorter pulses would deteriorate spectral selectivity [if $\tau_p \ll 1/\Omega_R$, then $\varrho_{if} \sim (\lambda\mu_{if})^2$, as for weak pulses], which would result in a decrease of the amplitude of the oscillations in $S(T)$. Much longer pulses would be unable to create a vibrational wave packet in the excited electronic state.

Given the values of the transition dipole moments (see Table I), a maximal field intensity of $\approx 3.6 \times 10^{12}$ W/cm^2 is estimated for the simulation of signals of Figs. 2 and 3. Probing HeNe dimers via SPSP spectroscopy thus requires relatively short (several hundred fs) and moderately strong ($\sim 10^{12}$ W/cm^2) pulses with a photon energy of $\sim$20.6 eV. Free-electron lasers can provide such pulses [61,62] and several XUV PP experiments have been performed recently [63]. High harmonics generated with intense IR lasers also fulfill the above requirements [64,65]. Time-domain SPSP experiments may complement the existing arsenal of steady-state weak-pulse spectroscopic techniques which have been used to study rare-gas dimers [53].

Application of steady-state saturation spectroscopy to the HeNe dimer seems to be impractical. Two competing effects should be taken into account. On the one hand, the atom-atom distance in the states $n = 2,3,4$ is approximately twice the distance in the state $n = 1$ [see the wave functions $\Psi_n(R)$ depicted in Fig. 1]. The states $n = 2,3,4$ thus have nearly four times larger collision cross sections and collisional quenching

rates than the state $n = 1$. On the other hand, the lifetime of the state $n = 1$ is three orders of magnitude shorter than those of the states $n = 2,3,4$. Therefore, the transition with strong μ_{01} saturates much faster than the transitions with small μ_{0n} ($n = 2,3,4$), rendering information on weak transitions very difficult to extract.

VIII. DISCUSSION AND CONCLUSIONS

We demonstrated that SPSP spectroscopy can be employed to effectively amplify weak transitions. As an illustration, we considered the possibility of detection of transitions to discrete vibrational states belonging to the [He($2\,^1S$)-Ne] 0^+ excited electronic state of the HeNe dimer.

Time-domain spectroscopy is usually applied to the monitoring of fast processes. The aim of SPSP spectroscopy for amplifying weak transitions is different: to visualize the frequencies of weak transitions as beatings in the time domain. The time-domain SPSP spectroscopy may be superior to steady-state saturation spectroscopy if weak and strong transitions overlap spectrally, or if weak transitions involve short-lived excited states and are thus significantly broadened, or if other sources of line broadening (e.g., collisions) are important. In addition, the use of short laser pulses may be dictated by the lack of suitable intense cw light sources with suitable photon energy.

The method of enhancement of weak transitions by SPSP spectroscopy is not limited to the specific system considered here. It can be applied to any system with discrete levels. On the one hand, weak transitions and (nearly) dark states are ubiquitous in polyatomic molecules. On the other hand, tunable sub-50-fs optical pulses are nowadays available from mid-infrared to ultraviolet [66], while free-electron lasers [67] or high-harmonic generation [65] offer intense 10–100 fs pulses in XUV. This suggests possible applications of SPSP spectroscopy to a variety of material systems.

Considering the application of SPSP spectroscopy, one has to estimate the contributions of unwanted processes like excited-state absorption, absorption of neighboring electronic states, multiphoton processes, photoionization, and photodissociation. Their contributions can be diminished by tuning the pump and probe pulses into resonance with the specific transitions to be interrogated or by utilizing pulses with purposefully designed shapes [68]. If the material system is properly selected and the experiment is carefully designed, the collective effect of these unwanted processes should not overwhelm the useful signal.

ACKNOWLEDGMENTS

This work has been supported by the Deutsche Forschungsgemeinschaft (DFG) through a research grant and the DFG-Cluster of Excellence "Munich-Centre for Advanced Photonics" (www.munich-photonics.de). A.K.B. gratefully acknowledges financial support from the Russian Foundation for Basic Research (Grant No. 13-03-00163-a). We thank Sergy Grebenshchikov for fruitful discussions.

APPENDIX: STRONG-PULSE DW OPERATORS

Let $G_a(t,t')$ be the time-evolution operators for the Liouville–von Neumann equation (8) in the case of $\lambda_2 = 0$ ($a = 1$) and $\lambda_1 = 0$ ($a = 2$):

$$\rho(t) \equiv G_a(t,t')\rho(t'). \tag{A1}$$

Then, the strong-pulse DW operators are given by [58]

$$D = G_1(\Delta, -\Delta)|0\rangle\langle 0|, \tag{A2}$$

$$W = \int_{-\Delta}^{\Delta} dt\, \mathcal{E}_2^*(t) X^\dagger G_2(t, -\Delta). \tag{A3}$$

Equations (A2) and (A3) assume that the arrival times for pulses 1 and 2 are set to zero ($\tau_a = 0$). $[-\Delta,\Delta]$ is a time interval outside of which the action of the pulse can be neglected. In our calculations, we took $\Delta = 3\tau_p$.

[1] S. Mukamel, *Principles of Nonlinear Optical Spectroscopy* (Oxford University, New York, 1995).
[2] R. P. Lucht, R. Trebino, and L. A. Rahn, Phys. Rev. A **45**, 8209 (1992).
[3] W. Kuehn, K. Reimann, M. Woerner, and T. Elsaesser, J. Chem. Phys. **130**, 164503 (2009).
[4] J. C. Wright, Annu. Rev. Phys. Chem. **62**, 209 (2011).
[5] P. Nuernberger, T. Vieille, C. Ventalon, and M. Joffre, J. Phys. Chem. B **115**, 5554 (2011).
[6] L. Allen and J. H. Eberly, *Optical Resonance and Two-Level Atoms* (Dover, New York, 1987).
[7] T. W. Hänsch, I. S. Shahin, and A. L. Schawlow, Phys. Rev. Lett. **27**, 707 (1971).
[8] J. L. Hall and C. J. Bordé, Phys. Rev. Lett. **30**, 1101 (1973).
[9] V. S. Letokhov and V. P. Chebotaev, Sov. Phys. Usp. **17**, 467 (1975).
[10] S. Svanberg, G.-Y. Yan, T. P. Duffey, W.-M. Du, T. W. Hänsch, and A. L. Schawlow, J. Opt. Soc. Am. B **4**, 462 (1987).
[11] R. W. Boyd and M. Sargent III, J. Opt. Soc. Am. B **5**, 99 (1988).
[12] J. Ishikawa, F. Riehle, J. Helmcke, and C. J. Bordé, Phys. Rev. A **49**, 4794 (1994).
[13] A. L. Schawlow, Rev. Mod. Phys. **54**, 697 (1982).
[14] T. W. Hänsch, Rev. Mod. Phys. **78**, 1297 (2006).
[15] R. L. Farrow and D. J. Rakestraw, Science **257**, 1894 (1992).
[16] D. S. Green, T. G. Owano, S. Williams, D. G. Goodwin, R. N. Zare, and C. H. Kruger, Science **259**, 1726 (1993).
[17] T. A. Reichardt and R. P. Lucht, J. Chem. Phys. **111**, 10008 (1999).
[18] K. Bultitude, R. Braftalean, and P. Ewart, J. Raman Spectrosc. **34**, 1030 (2003).
[19] M. Kirste, X. Wang, G. Meijer, K. B. Gubbels, Ad van der Avoird, G. C. Groenenboom, and S. Y. T. van de Meerakker, J. Chem. Phys. **137**, 101102 (2012).
[20] T. Frohnmeyer, M. Hofmann, M. Strehle, and T. Baumert, Chem. Phys. Lett. **312**, 447 (1999).

[21] J. González-Vazquez, L. González, S. Nichols, T. Weinacht, and T. Rozgonyi, Phys. Chem. Chem. Phys. **12**, 14203 (2010).
[22] M. F. Gelin, C. Riehn, M. Kunitski, and B. Brutschy, J. Chem. Phys. **132**, 134301 (2010).
[23] T. Buckup, J. Hauer, C. Serrat, and M. Motzkus, J. Phys. B **41**, 074024 (2008).
[24] I. Gerhardt, G. Wrigge, G. Zumofen, J. Hwang, A. Renn, and V. Sandoghdar, Phys. Rev. A **79**, 011402 (2009).
[25] A. P. Conde, R. Montero, A. Longarte, and F. Castano, Phys. Chem. Chem. Phys. **12**, 15501 (2010).
[26] T. Bittner, K. D. Irrgang, G. Renger, and M. R. Wasielewski, J. Phys. Chem. **98**, 11821 (1994).
[27] O. A. Sytina, V. I. Novoderezhkin, R. van Grondelle, and M. L. Groot, J. Phys. Chem. A **115**, 11944 (2011).
[28] M. W. Graham, Y. Z. Ma, and G. R. Fleming, Nano Lett. **8**, 3936 (2008).
[29] D. B. Turner and K. A. Nelson, Nature **466**, 1089 (2010).
[30] T. Renger, V. May, and O. Kühn, Phys. Rep. **343**, 137 (2001).
[31] C. P. Koch, T. Klüner, and R. Kosloff, J. Chem. Phys. **116**, 7983 (2002).
[32] Y. Tanimura and Y. Maruyama, J. Chem. Phys. **107**, 1779 (1997).
[33] O. Kühn, Y. Zhao, F. Shuang, and Y. J. Yan, J. Chem. Phys. **112**, 6104 (2000).
[34] H. Wang and M. Thoss, J. Chem. Phys. **124**, 034114 (2006).
[35] M. Machholm and A. Suzor-Weiner, J. Chem. Phys. **105**, 971 (1996).
[36] M. F. Gelin, D. Egorova, and W. Domcke, J. Chem. Phys. **131**, 124505 (2009).
[37] M. F. Gelin, D. Egorova, and W. Domcke, J. Phys. Chem. Lett. **2**, 114 (2011).
[38] M. F. Gelin, D. Egorova, and W. Domcke, Phys. Chem. Chem. Phys. **15**, 8119 (2013).
[39] B. Brüggemman, P. Kjellberg, and T. Pullerits, Chem. Phys. Lett. **444**, 192 (2007).
[40] D. Abramavicius, Y.-Z. Ma, M. W. Graham, L. Valkunas, and G. R. Fleming, Phys. Rev. B **79**, 195445 (2009).
[41] R. P. Lucht, P. J. Kinnius, S. Roy, and J. R. Gord, J. Chem. Phys. **127**, 044316 (2007).
[42] G. Gerullo, C. J. Bardeen, Q. Wang, and C. V. Shank, Chem. Phys. Lett. **262**, 362 (1996).
[43] C. J. Bardeen, V. V. Yakovlev, K. R. Wilson, S. D. Carpenter, P. M. Weber, and W. S. Warren, Chem. Phys. Lett. **280**, 151 (1997).
[44] J. Schneider, M. Wollenhaupt, A. Winzenburg, T. Bayer, J. Köhler, R. Faust, and T. Baumert, Phys. Chem. Chem. Phys. **13**, 8773 (2011).
[45] H. Rabitz, R. de Vivie-Riedle R, M. Motzkus and K.-L. Kompa, Science **288**, 824 (2000).
[46] P. Nuernberger, G. Vogt, T. Bixner, and G. Gerber, Phys. Chem. Chem. Phys. **9**, 2470 (2007).
[47] M. Wollenhaupt and T. Baumert, Faraday Discuss. **153**, 9 (2011).
[48] K. Ohmori, Annu. Rev. Phys. Chem. **60**, 487 (2009).
[49] B. D. Bruner, H. Suchowski, N. V. Vitanov, and Y. Silberberg, Phys. Rev. A **81**, 063410 (2010).
[50] V. I. Prokhorenko, A. Halpin, P. J. M. Johnson, R. J. D. Miller, and L. S. Brown, J. Chem. Phys. **134**, 085105 (2011).
[51] R. Hildner, D. Brinks, F. D. Stefani, and N. F. van Hulst, Phys. Chem. Chem. Phys. **13**, 1888 (2011).
[52] D. Brinks, R. Hildner, F. D. Stefani, and N. F. van Hulst, Faraday Discuss. **153**, 51 (2011).
[53] G. N. Gerasimov, Phys. Usp. **47**, 149 (2004).
[54] J. F. Ogilive and F. Y. H. Wang, J. Mol. Struct. **291**, 313 (1993).
[55] S. M. Cybulski and R. R. Toczylowski, J. Chem. Phys. **111**, 10520 (1999).
[56] R. J. Buenker, H. P. Liebermann, and A. Z. Devdariani, J. Phys. Chem. A **111**, 1307 (2007).
[57] A. Z. Devdariani, A. K. Belyaev, A. B. Alekseev, H. P. Liebermann, and R. J. Buenker, Mol. Phys. **108**, 757 (2010).
[58] M. F. Gelin, D. Egorova, and W. Domcke, J. Phys. Chem. B **115**, 5648 (2011).
[59] A. Z. Devdariani, A. K. Belyaev, A. B. Alekseev, H. P. Liebermann, and R. J. Buenker, Russian J. Phys. Chem. B **5**, 952 (2011).
[60] A. P. Blokhin, M. F. Gelin, I. I. Kalosha, S. A. Polubisok, and V. A. Tolkachev, J. Chem. Phys. **110**, 978 (1999).
[61] T. Shintake *et al.*, Nat. Photon. **2**, 555 (2008).
[62] A. Rudenko *et al.*, J. Phys. B **43**, 194004 (2010).
[63] M. Magrakvelidze *et al.*, Phys. Rev. A **86**, 013415 (2012).
[64] P. Villoresi, P. Ceccherini, L. Poletto, G. Tondello, C. Altucci, R. Bruzzese, C. de Lisio, M. Nisoli, S. Stagira, G. Cerullo, S. De Silvestri, and O. Svelto, Phys. Rev. Lett. **85**, 2494 (2000).
[65] K. Midorikawa, Y. Nabekawa, and A. Suda, Prog. Quantum Electron. **32**, 43 (2008).
[66] U. Megerle, I. Pugliesi, C. Schriever, C. F. Sailer, and E. Riedle, Appl. Phys. B **96**, 215 (2009).
[67] J. Ullrich, A. Rudenko, and R. Moshammer, Annu. Rev. Phys. Chem. **63**, 635 (2012).
[68] J. P. Palao, R. Kosloff, and C. P. Koch, Phys. Rev. A **77**, 063412 (2008).